Comparison of Monthly IMERG Precipitation Estimates with PACRAIN Atoll Observations

DAVID T. BOLVIN,[a,b] GEORGE J. HUFFMAN,[a] ERIC J. NELKIN,[a,b] AND JACKSON TAN[a,c]

[a] *Laboratory for Atmospheres, NASA GSFC, Greenbelt, Maryland*
[b] *Science Systems and Applications, Inc., Lanham, Maryland*
[c] *Universities Space Research Association, Columbia, Maryland*

(Manuscript received 13 August 2020, in final form 21 April 2021)

ABSTRACT: Satellite-based precipitation estimates provide valuable information where surface observations are not readily available, especially over the large expanses of the ocean where in situ precipitation observations are very sparse. This study compares monthly precipitation estimates from the Integrated Multisatellite Retrievals for GPM (IMERG) with gauge observations from 37 low-lying atolls from the Pacific Rainfall Database for the period June 2000–August 2020. Over the analysis period, IMERG estimates are slightly higher than the atoll observations by 0.67% with a monthly correlation of 0.68. Seasonally, DJF shows excellent agreement with a near-zero bias, while MAM shows IMERG is low by 4.6%, and JJA is high by 1.2%. SON exhibits the worst performance, with IMERG overestimating by 6.5% compared to the atolls. The seasonal correlations are well contained in the range 0.67–0.72, with the exception of SON at 0.62. Furthermore, SON has the highest RMSE at 4.70 mm day^{-1}, making it the worst season for all metrics. Scatterplots of IMERG versus atolls show IMERG, on average, is generally low for light precipitation accumulations and high for intense precipitation accumulations, with best agreement at intermediate rates. Seasonal variations exist at light and intermediate rate accumulations, but IMERG consistently overestimates at intense precipitation rates. The differences between IMERG and atolls vary over time but do not exhibit any discernable trend or dependence on atoll population. The PACRAIN atoll gauges are not wind-loss corrected, so application of an appropriate adjustment would increase the precipitation amounts compared to IMERG. These results provide useful insight to users as well as valuable information for future improvements to IMERG.

KEYWORDS: Precipitation; In situ oceanic observations; Satellite observations; Tropics; Rainfall; Pacific Ocean; Gauges

1. Introduction

The accurate quantification of precipitation over land is crucial in supporting the monitoring of short-term events such as flood prediction, landslide modeling, and crop management and long-term phenomena such as droughts and resource planning. Because the land–ocean atmospheric system is intricately linked, it is equally important to quantify the distribution of precipitation over ocean to understand such phenomena as El Niño, the Madden–Julian oscillation, and atmospheric rivers, as well as the global energy and water cycle. Rain gauges have been the vanguard of precipitation observation, but coverage over land is sparse in much of the world (Kidd et al. 2017) and even more sparse over open ocean. Over the last several decades, satellite-based precipitation estimates have proven extremely useful in providing excellent spatial and temporal coverage not available with surface observations. As satellite estimates are based on indirect observation of precipitation at the satellite footprint size, they need to be validated, to the extent possible, against available surface observations to assess quality. Numerous studies have validated various satellite-based precipitation estimation algorithms over land using dense rain gauge observations and radar-based estimates. However, validation efforts over open ocean are far more challenging due to the unique environment of ocean-based in situ observations. Ocean-based buoy gauge arrays such as the Pacific Ocean Tropical Atmosphere Ocean (TAO)/TRITON (McPhaden 1995), the Atlantic Prediction and Research Moored Array in the Tropical Atlantic (PIRATA; Bourlès et al. 2008), and the Indian Ocean–Research Moored Array for African–Asian–Australian Monsoon Analysis and Prediction (RAMA; McPhaden et al. 2009) have issues compared to traditional land-based rain gauges, such as frequent interruptions in temporal coverage, wind effects, potential sea spray contamination, and loss due to piracy. In addition to buoys, ship-based observations such as those provided by the Ocean Rainfall and Ice-Phase Precipitation Measurement Network (OceanRAIN; Klepp 2015; Klepp et al. 2017) are available but provide only a single gauge that changes location in time, making extended validation for any given region a challenge.

Due to the inherent limitations of ocean-based gauge observations, alternative means of validating satellite-based precipitation estimates for extended time spans should be evaluated. One alternative is radar-based precipitation estimates collected from islands, or from ships involved in field campaigns, but both sources lack extensive time/space coverage. Low-lying atoll gauge stations, which can be considered a proxy for open ocean as land effects are minimized, provide a sparse but persistent network of stations. The Pacific Rainfall Database (PACRAIN) dataset provides a long record of quality-controlled atoll gauge observations well suited for use in validating satellite-based precipitation estimates in the tropical Pacific region (Cook and Green 2019; Greene et al. 2008). The PACRAIN dataset also contains "low" and "high" island stations, but we follow the established practice of

Corresponding author: David T. Bolvin, david.t.bolvin@nasa.gov

DOI: 10.1175/JHM-D-20-0202.1

excluding them to avoid possible land heating and orographic effects that likely make them unrepresentative of the open ocean.

The goal of this study is to use monthly PACRAIN atoll gauge observations to provide initial validation of the oceanic precipitation estimates from the recently released version (V06B) of the Integrated Multisatellite Retrievals for Global Precipitation Measurement (GPM) mission (IMERG; Huffman et al. 2019, 2020), which is the U.S. merged-satellite algorithm for GPM, and covers the period from June 2000 to (delayed) present (where "delayed" is included to note that the latency of the IMERG product used in this analysis is about 3 months). The results of this analysis provide insight into the quality of IMERG V06B monthly estimates over open ocean, with the intent to use this validation information to improve future versions of IMERG. Some previous studies have assessed the quality of earlier versions of the IMERG estimates over ocean. Kucera and Klepp (2017) found that IMERG Version 03 underestimated precipitation compared to shipborne OceanRAIN optical disdrometer observations, especially in convective tropical rainfall for the period March 2014–January 2016. Khan and Maggioni (2019) showed IMERG Version 05 also underestimated precipitation compared to OceanRAIN observations for the period March 2014–February 2017. Wu and Wang (2019) evaluated IMERG V05 against buoy gauges in the Pacific, Atlantic, and Indian Oceans, finding that both underestimation and overestimation occurs depending on gauge location and precipitation intensity. As V06B is a major overhaul compared to previous versions, it is important to continue validation efforts, over both land and ocean.

This paper describes the results of the comparison between the IMERG V06B Final monthly estimates and the PACRAIN atoll gauge observations for the period June 2000–August 2020. The IMERG and PACRAIN datasets are described in section 2, and the analysis methodology is outlined in section 3. Section 4 provides the comparison results and section 5 presents a discussion of the results as well as conclusions.

2. Datasets

a. IMERG version 06B monthly estimates

IMERG is the U.S. merged-satellite algorithm for the GPM mission and is a code-level merger of major components from three preexisting state-of-the-art satellite precipitation algorithms: the Kalman-filter-based Climate Prediction Center (CPC) morphing technique (KF-CMORPH; Joyce et al. 2004; Joyce et al. 2011), the Precipitation Estimation from Remotely Sensed Information Using Artificial Neural Networks–Cloud Classification System (PERSIANN-CCS; Hong et al. 2004), and the Tropical Rainfall Measuring Mission (TRMM) Multisatellite Precipitation Analysis (TMPA; Huffman et al. 2007, 2010). Specifically, IMERG uses the quasi-Lagrangian propagation of passive microwave (PMW) precipitation estimates and the Kalman filter estimation features from KF-CMORPH, and the cloud classification technique PERSIANN-CCS to estimate geostationary infrared (geoIR)-based precipitation. TMPA provided the precipitation gridding, intercalibration, and merging components of IMERG to create the satellite-only estimates, as well as the satellite–gauge merging technique. The goal of IMERG is to create a unified algorithm that maximizes the strengths of each individual algorithm in an attempt to produce a single, best estimate of precipitation at the half-hourly and monthly temporal resolution and the $0.1° \times 0.1°$ spatial resolution. Though IMERG is a merger of components from preexisting algorithms, it is important to note that many enhancements and improvements have been implemented since the first operational version (V03), introduced shortly after the launch of the GPM satellite in February 2014. In common with prior versions, IMERG V06B consists of three distinct Runs with different latencies for different applications—Early, Late, and Final. The Early and Late Runs are available 4 and 14 h after real time, respectively, and are intended for real-time monitoring applications. The Final Run, available 3 months after real time, is used for research purposes. All three runs produce half-hourly precipitation estimates, but only the Final Run (which is used in this study) produces a monthly merged satellite–gauge estimate.

The IMERG V06B record currently covers the period from June 2000 to (delayed) present using the TRMM and GPM core satellites over their respective periods to calibrate the PMW precipitation estimates from the constellation of available partner satellites. The goal is to maintain a homogeneous precipitation record despite changes in the partner satellite constellation over time, as well as the change in the calibration satellite from TRMM to GPM in 2014. Despite the best effort to maintain homogeneity, IMERG is considered a high-resolution precipitation product, which provides the highest-quality snapshot precipitation estimate, and not a climate data record, which stresses homogeneity over snapshot accuracy (Gehne et al. 2016). The TRMM era of IMERG spans June 2000–May 2014 and the GPM era spans from June 2014 to (delayed) present (August 2020 in this study), with the objective of maintaining homogeneity across the calibration boundary.

To summarize the parts of IMERG processing relevant to this study, the first step is to convert brightness temperatures to precipitation estimates using the Goddard profiling algorithm (GPROF2017; Kummerow et al. 1998, 2001, 2015) for all PMW sensors, with the exception of the Sounder for Probing Vertical Profiles of Humidity (SAPHIR) instrument which is processed using the Precipitation Retrieval and Profiling Scheme (PRPS; Kidd 2018). Over ocean, the PMW retrievals make use of all the channels on a given sensor. During the TRMM era, the gridded partner satellite precipitation estimates are first calibrated to the TRMM Microwave Imager (TMI) estimates, and then calibrated to the combined PR/TMI product (CORRA-T; Grecu et al. 2016). In the GPM era the partner satellite estimates are first calibrated to the GPM Microwave Imager (GMI) product, and then calibrated to the combined DPR/GMI Ku-band product (CORRA; Grecu et al. 2016). This two-step procedure is necessary as direct calibration of the partner satellites against the narrow Ku-swath CORRA and CORRA-T lacks sufficient sampling to obtain a stable calibration. The individual intercalibrated PMW precipitation estimates are then

selectively merged into half-hour increments at 0.1° spatial resolution. As satellite coverage for any given half-hour is sparse, Final Run IMERG propagates the PMW precipitation from past (forward propagation) and future (backward propagation) estimates using precipitation motion vectors to obtain global coverage every half hour (Tan et al. 2019). In V06B, precipitation motion vectors are computed by tracking motions in successive fields of total column water vapor from the Modern-Era Retrospective Analysis for Research and Applications, version 2 (MERRA-2; Gelaro et al. 2017), for the Final Run.

Half-hourly geoIR-based precipitation estimates are also computed by applying PERSIANN-CCS to the CPC 4-km IR brightness temperature data and calibrating the results to the merged PMW estimate. Since propagated PMW estimates lose skill within a few hours, these IR-based estimates have skill and provide valuable information when there are several-hour time gaps between the PMW satellite overpasses. The satellite-observed PMW precipitation, the forward- and backward-propagated PMW precipitation, and the geoIR-based precipitation estimates are then combined within a Kalman filter framework to produce a global precipitation field every half hour (with limitations at high latitudes). The monthly Final Run datasets used in this study merge the monthly Legates–Willmott wind-loss corrected (Legates 1987) Global Precipitation Climatology Centre (GPCC) Monitoring (Schneider et al. 2018a) or Full (Schneider et al. 2018b) gauge analysis, depending on availability, with the monthly satellite-only estimate using inverse error weighting. The Full Product Version 2016 covers June 2000–December 2016, and the Monitoring Product Version 6 covers January 2017 to (delayed) present. In this study, the monthly IMERG V06B Final Run is validated against the atoll observations.

b. *PACRAIN atoll daily observations*

The PACRAIN dataset, created and maintained by the University of Oklahoma, consists of daily and monthly gauge observations from Pacific coastal and inland island stations, as well as low-lying atoll stations, covering the period from January 1874 to (delayed) present. Input sources consist of the New Zealand National Institute of Water and Atmospheric Research, the French Polynesian Meteorological Service, the U.S. National Centers for Environmental Information, the Schools of the Pacific Rainfall Climate Experiment (Postawko et al. 1994), and ''An atlas of Pacific islands rainfall'' (Taylor 1973). The database currently consists of 965 stations that cover the region 30°S–28°N, 131°E–130°W, and is updated with new observations at the beginning of each month, including updates to correct for newly discovered errors performed on an as-needed basis. For uniformity, the reporting time for each station is given as the UTC start time of the accumulation period. The PACRAIN observations provide uniform metadata and are rigorously quality controlled to ensure accurate reporting times which can vary widely depending on the source. It is important to note that the complement of stations varies significantly from month to month and there is no guarantee of continuity for any single station within the record. In this analysis, only the atoll stations are used as they best represent open ocean observations. It should be noted that the 1° GPCC analyses contain island stations, but the gauge adjustment is limited to IMERG pixels over land to avoid biasing the IMERG ocean estimates. Although PACRAIN atoll stations may be included in the GPCC analyses, all such data are audited out of the IMERG analysis. Furthermore, no wind-loss correction has been applied to the PACRAIN gauge observations. The PACRAIN atoll station processing procedure is detailed in section 3.

3. Analysis methodology

IMERG V06B Final Run estimates and PACRAIN atoll station observations are compared at the monthly, 0.1° resolution for the period June 2000–August 2020, the most recent month of PACRAIN atoll data available at the time of this analysis. Monthly atoll accumulations are computed from the daily PACRAIN observations and then compared at the monthly scale with the IMERG estimates. Daily atoll stations that fall within the analysis span are identified along with the corresponding UTC observation times. Due to the nature of the PACRAIN observations, it is unlikely that any one atoll will cover the entire analysis record, so any atoll observation that falls within the analysis span is considered. In the process of computing the monthly atoll accumulations, the candidate stations are checked to ensure that (i) there are no days missing for a given month, (ii) the accumulation span does not exceed 24 h, and (iii) observations do not contain negative values; otherwise, they are removed. The vast majority of atoll months were removed due to missing days. Due to the ''weekend effect'' and other reasons, accumulation periods can exceed 24 h. These multiday accumulations are generally atypical and excluded for computational efficiency. For reasons unknown to the authors, atoll stations occasionally have negative daily precipitation rates, which likely indicates a missing observation. It should be noted that atoll observation times can change, but these changes are rare and do not affect the monthly accumulations. In total, days with precipitation less than −1 and accumulation periods greater than 24 h each account for a 4% reduction in the number of atoll months, while months with missing days account for the remaining 92% reduction in number of atoll months. Due to the screening criteria, more than 50% of the PACRAIN atoll months were removed by the quality assurance procedure. As a result, a total of 37 atoll stations that met the quality control criteria for at least one month during the analysis period were identified and used.

Because the atoll reporting times vary from station to station, they do not necessarily conform to the definition of the IMERG monthly product, which starts at 0000:00 UTC on the first day of the month and ends on 2359:59 UTC of the last day of the month. Therefore, atoll observations that cross the day boundary of the first and last day of the month must be accommodated when computing the monthly total. Thus, if the reporting time of the station on the last day of the previous month is >1200 UTC, it is included in the current monthly total. If the reporting time of the station is ≤1200 UTC on the last day of the current month it is included in the monthly total.

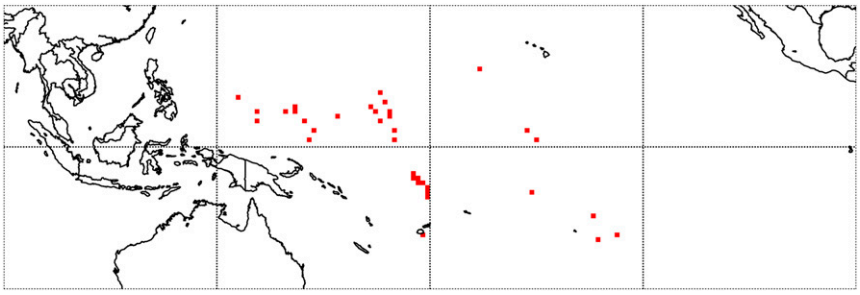

FIG. 1. Atoll station locations (red squares) used in this analysis. Depicted at 1° for display purposes.

This scheme may misassign precipitation to the first and last day of the month, but it is expected that the 1200 UTC cutoff will minimize the monthly accumulation errors. An alternative scheme is to assume a constant precipitation rate for those days that straddle the beginning and end of the month and prorate the amount of rain based on the number of hours in the day that fall within the month of interest. This approach forces the begin and end days to contribute to the monthly total regardless of when the precipitation occurred during these days. The relative merits of the two options have not been exhaustively examined as they both have advantages and disadvantages, so the former approach was chosen as the standard aggregation method.

Figure 1 shows the locations of the 37 PACRAIN atoll stations used in the analysis (red squares). For visualization purposes, the locations are shown at the 1° resolution, and thus a few red squares contain more than one atoll station. While the atoll stations are fairly well distributed in space with most gauges occupying a separate 0.1° grid box, the number of stations reporting for any given month can vary widely. Figure 2 shows the time series of the number of contributing atoll stations for the analysis period. Early in the period there are a maximum of 17 atoll stations contributing to the month, with several later months having no atoll observations that meet the quality control criteria. Most notably, this occurs for several months in 2013. Though the record has inhomogeneities in coverage, it is believed that the results using a long analysis period are sufficiently stable, eliminating the necessity of weighting each month by the number of contributing atoll stations. A final issue is whether the atoll "point" gauge statistics are comparable to those of the IMERG 0.1° grid boxes. At the monthly scale, the correlation distances for gauges are much larger than 0.1°. Bell and Kundu (2003) showed that correlation

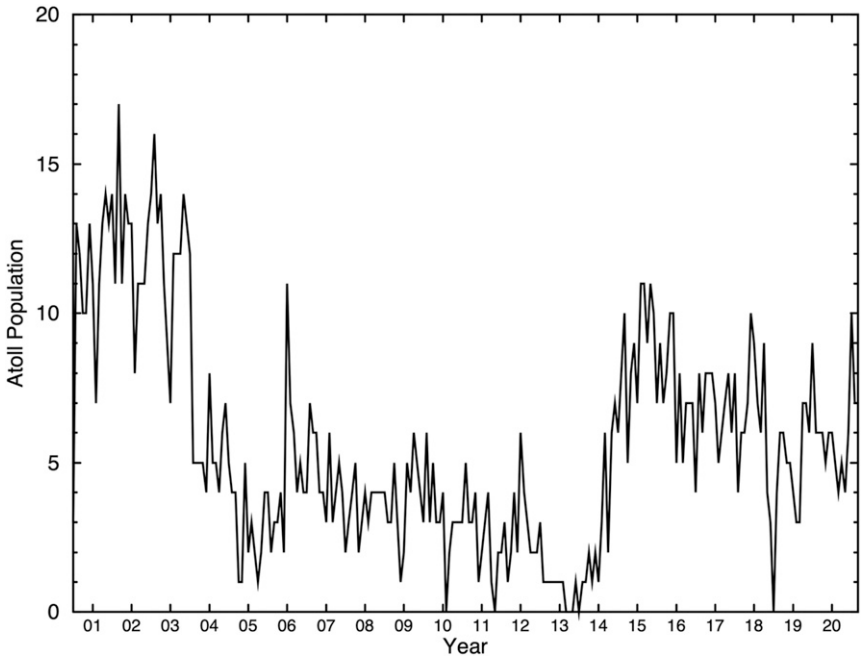

FIG. 2. Time series of the number of monthly atoll stations for the analysis period June 2000–August 2020.

TABLE 1. Comparison of monthly IMERG estimates and atoll observations for the period June 2000–August 2020 aggregated by all months and individual seasons. Bold indicates the best result, and italics indicates the worst result.

	Atoll mean (mm day^{-1})	IMERG mean (mm day^{-1})	Bias (mm day^{-1})	Percent bias	Correlation	RMSE (mm day^{-1})	No. of samples
All seasons	9.08	9.15	+0.06	+0.67	0.68	4.52	1375
DJF	8.94	8.94	**+0.005**	**+0.06**	**0.72**	4.63	327
MAM	9.46	9.02	−0.44	−4.6	0.71	4.54	348
JJA	9.03	9.14	+0.11	+1.2	0.67	**4.24**	367
SON	8.90	9.48	*+0.58*	*+6.5*	*0.62*	*4.70*	333

distances for gauges are on the order of hundreds of kilometers for monthly accumulations, while Morrissey (1991) showed the PACRAIN atolls have a correlation distance on the order of 500 km, ensuring valid comparisons can be performed between the ''point'' atoll gauges and the gridded IMERG estimates.

4. Comparison results

Monthly IMERG estimates from the Final Run are compared with the monthly atoll observations gridded at the 0.1° resolution for the span June 2000–August 2020 for the entire period as well as by season. The metrics used to assess IMERG are bias (IMERG minus atoll gauge), percent bias (bias divided by atoll gauge × 100), correlation, and root-mean-square error (RMSE). Table 1 shows the overall and seasonal comparison statistics between the monthly IMERG estimates and the atoll observations. For the entire analysis span, the IMERG average is slightly high compared to the atolls by 0.67%, with a correlation of 0.68 and an RMSE of 4.52 mm day^{-1}. Defining the four 3-month seasons December–February (DJF), March–May (MAM), June–August (JJA), and September–November (SON), we find that IMERG and the atolls both have nearly constant seasonal averages varying by approximately 5.9% and 6.1%, respectively. The low seasonal variations in the means are interesting given the dynamic nature of the western Pacific seasonal climatology and the static locations of the atoll gauges. IMERG and the atolls agree best in DJF in terms of bias (+0.005 mm day^{-1}) and percent bias (+0.06%), and have the best correlation at 0.72. For MAM, IMERG underestimates by −4.6%, while JJA and SON overestimate by +1.2% and 6.5%, respectively. For all seasons except SON, the correlations are well contained with a range of 0.67–0.72. IMERG has the lowest RMSE in JJA at 4.24 mm day^{-1}, lower than that of DJF (4.63 mm day^{-1}) and MAM (4.54 mm day^{-1}). For every metric, IMERG performs the worst in SON with a bias, percent bias, correlation, and RMSE of +0.58 mm day^{-1}, +6.5%, 0.62, and 4.70 mm day^{-1}, respectively. All correlation coefficients are statistically significant with a two-tailed p value less than 0.001 based on a t test.

Figure 3 shows the scatterplot of IMERG estimates versus atoll observations in individual monthly grid boxes for the analysis period. The red line indicates the one-to-one line, and the green line is the corresponding quantile–quantile plot. IMERG clearly underestimates the atolls at monthly rates below 3 mm day^{-1}, with a gradual decrease in underestimation in the range 3–17 mm day^{-1}. Above 17 mm day^{-1}, IMERG accumulations increasingly overestimate the atoll observations on the average, which indicates that the overall overestimation by IMERG is the result of the most intense accumulated precipitation rates. Despite the low-end underestimation and the high-end overestimation, the overall bias is small, indicating that the under/overestimation differences show some level of compensation. Figures 4a–d depict the seasonal scatterplots of IMERG versus the atolls for DJF, MAM, JJA, and SON, respectively. In the broadest sense, the seasonal scatterplots echo the overall pattern shown in Fig. 3, but there are notable differences from season to season that lead to both rate-dependent over- and underestimation. Figure 4a shows DJF, which exhibits a modest underestimation at lower rates (0–2 mm day^{-1}) and approximate agreement between IMERG and the atolls in the range 2–17 mm day^{-1}, and general overestimation at rates above 17 mm day^{-1}. The overall differences indicate that, on average, IMERG and atolls have excellent agreement for DJF. Unlike DJF, MAM (Fig. 4b) shows IMERG consistently underestimates the atoll observations for all but the most intense rates, those above 26 mm day^{-1}. JJA and

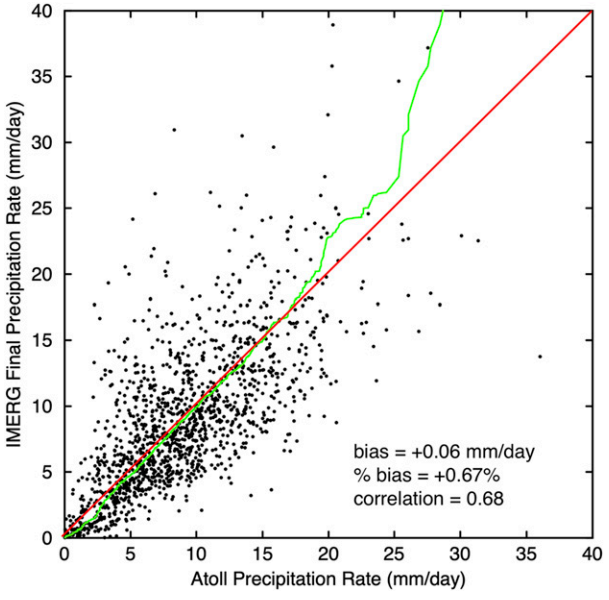

FIG. 3. Scatterplot of monthly IMERG estimates and atoll observations for the entire analysis period June 2000–August 2020. The green line depicts the quantile–quantile line, and the red line depicts the one-to-one line.

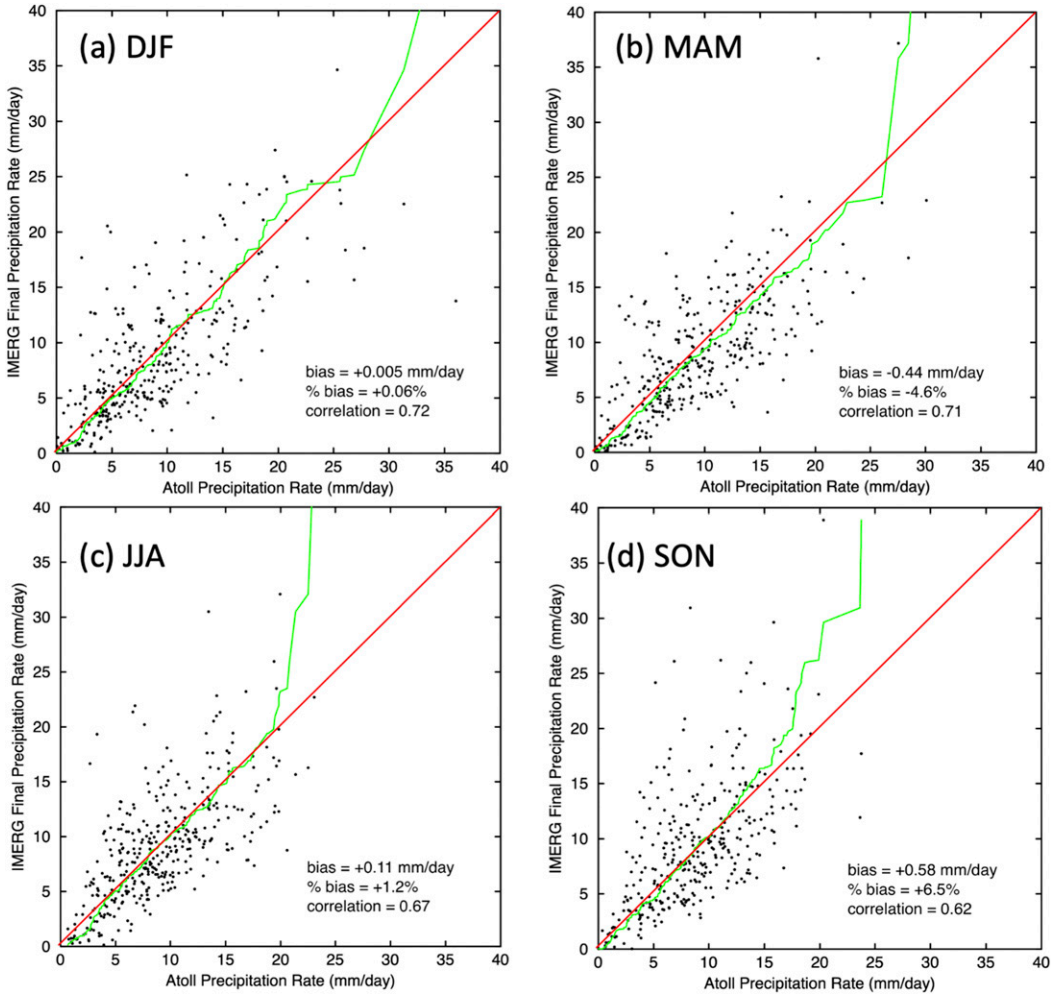

FIG. 4. As in Fig. 3, but for (a) December–February (DJF), (b) March–May (MAM), (c) June–August (JJA), and (d) September–November (SON).

SON, Figs. 4c and 4d, respectively, both show IMERG overestimates compared to the atoll observations, albeit to different degrees. Of all seasons, JJA tends to mimic the overall pattern shown in Fig. 3, with underestimation at rates up to 3 mm day^{-1}, overestimation above 17 mm day^{-1}, and reasonable agreement at intermediates rates. Furthermore, JJA shows the lowest RMSE at 4.24 mm day^{-1}. SON exhibits the largest differences between IMERG and the atolls with IMERG slightly underestimating at rates below 6 mm day^{-1}, having good agreement in the range 6–12 mm day^{-1}, and substantial overestimation above 12 mm day^{-1}. It is clear that the behavior of the IMERG estimates with respect to the atoll observations varies by season from the overall statistics, but the seasonal scatterplots do show similarities. Note that excursions in the seasonal quantile–quantile plots are dictated by a relatively few points at the most intense rain rates, but still show some degree of consistency.

To examine the temporal variations of the IMERG and atoll differences, Fig. 5 shows the time series of the IMERG monthly estimates and the atoll observations for the analysis span. As a result of the atoll availability and our quality control, there are gaps in the time series for months that contain no atoll observations. For those continuous spans with at least 14 months, 7-month running means were computed to remove high-frequency variability. The 7-month span was chosen as it provided the best trade-off between smoothness and applicability to the durations of available atoll time series segments. As shown by the 7-month running mean curves, there is no consistent overestimation by IMERG as a function of time and additionally, there is no discernible trend in the differences. Because the complement of atoll stations changes over time, there is the possibility that the IMERG and atoll comparisons are biased by the number of monthly atoll stations, which can vary between 0 and 17 over the record. To investigate this possibility, we computed the correlation between the time series of atoll population (Fig. 2) and the (IMERG minus atoll) difference in the average monthly precipitation rates computed from Fig. 5. The resulting correlation of 0.09 indicates that the changes in the atoll populations are

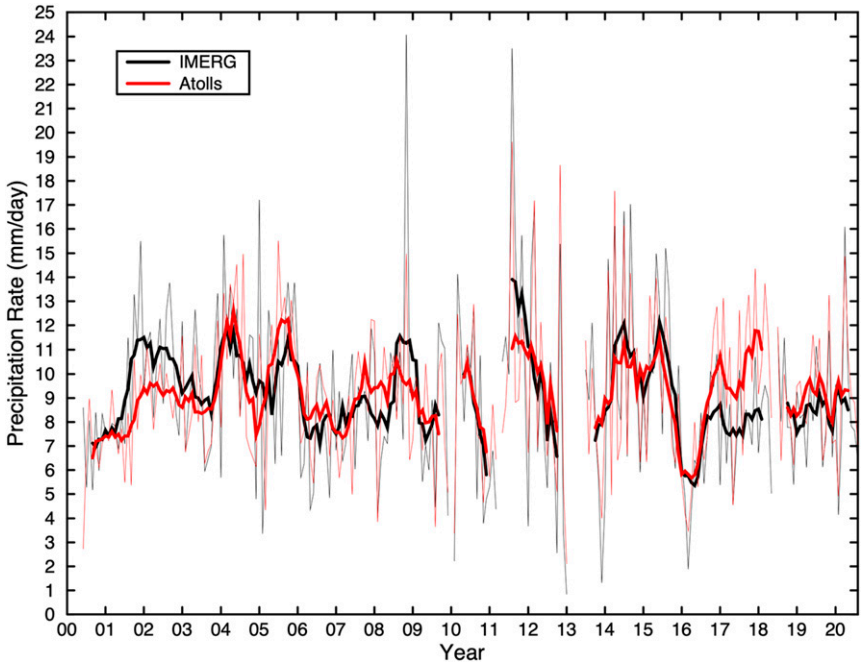

FIG. 5. Time series plot of monthly mean IMERG and atoll values for the period June 2000–August 2020. The thick lines indicate 7-month running means.

not a dominant factor in the month-to-month IMERG and atoll differences.

5. Discussion and conclusions

Monthly IMERG V06B precipitation estimates from the Final Run are validated against PACRAIN atoll observations for the period June 2000–August 2020. The goal of this study is to provide initial validation of the oceanic precipitation estimates from IMERG, primarily in terms of bias to determine how well the long-term mean of IMERG compares with the long-term mean of the atolls. Furthermore, the results of this analysis provide information regarding the quality of the IMERG V06B monthly estimates that will lead to direct improvements to future versions of IMERG. Over the entire period, IMERG slightly overestimates monthly precipitation compared to atoll gauge observations by 0.67%. At accumulated light rain rates, IMERG is consistently low compared to atolls, which is likely the result of satellite detectability issues for light or small precipitation systems as satellite footprint sizes are on the order of 5–25 km while the gauge is a point measurement. As a result, atoll gauges will observe smaller precipitation events that satellite retrievals may not be able to resolve. Note that this underestimation is not specific to IMERG, but rather is endemic to satellite-based precipitation estimates in general. As there is reasonably good agreement between IMERG and atolls at accumulated intermediate precipitation rates, the more intense accumulated rain rates in IMERG drive the overall positive bias. Though the general shape of seasonal scatterplots is similar to that for the overall period, the deviations dictate the seasonal extent of the IMERG over/underestimation. For example, all seasonal plots show varying degrees of underestimation at light rates, most notably JJA. With the exception of MAM where IMERG underestimates for all but the most intense rates, the intermediate rates for each season tend to show reasonable agreement. One feature common to all plots is that IMERG overestimates precipitation at the most intense rates, the degree of which varies by season. For comparison, Kucera and Klepp (2017) found that IMERG V03 underestimated intense precipitation in the tropics, whereas IMERG V06B overestimates intense precipitation, the result of significant algorithm changes from V03 to V06B. Like V03, Khan and Maggioni (2019) showed that IMERG V05 also underestimated precipitation, though the study area was not confined to the tropics. In the tropics, Wu and Wang (2019) found IMERG V05 both underestimated and overestimated precipitation, depending on gauge location and precipitation intensity. From these results, it can be inferred that V06B has a higher occurrence of intense precipitation rates compared to previous versions of IMERG.

As the degree of over/underestimation by IMERG varies by season, there is strong indication that the interseasonal differences are dependent on climatological precipitation regime, which can be quite dynamic, and the location of the atoll stations which are spread over a large area of the central and western Pacific. For example, it is likely that the high percent bias in SON is influenced by more intense rain rates from typhoons, as there are a large number of atolls within the SON Pacific typhoon track. On the other hand, the JJA Pacific typhoon track is farther west, where there are fewer atolls, leading to a smaller bias. In DJF, the comparisons are good

despite a climatological shift of the South Pacific convergence zone toward the atoll region. The underestimation in MAM is the likely the result of the weaker South Pacific convergence zone and narrowing of the intertropical convergence zone. Therefore, it appears that the locations of the atolls play a large role in determining the degree of bias of IMERG due to the seasonal evolution of the intertropical convergence zone, South Pacific convergence zone, and tropical cyclone tracks. Further stratification of IMERG rain rates as a function of atoll location and season would be necessary to study the regime dependency in more detail, but that is beyond the scope of this analysis. In addition, analysis comparing daily IMERG estimates with daily atoll observations would bypass some limitations associated with monthly comparisons, and constitute a topic of future work. The overestimation of IMERG at more intense precipitation rates is currently a subject of investigation by the IMERG development team. Previous studies using earlier versions of IMERG indicated consistent underestimation over ocean, but not necessarily in the same region as the current analysis. Furthermore, changes in the intercalibration of sensors in IMERG V06 may have led to a change in the bias. Therefore, focusing on the algorithm changes in IMERG V06B compared to earlier versions is helpful to diagnosing this overall shift.

Noted earlier, the IMERG Final Run applies the Legates–Willmott wind-loss correction to the GPCC gauge analyses prior to merging with the monthly satellite-only estimate to account for undercatch. As part of the GPCC gauge–satellite-only merger process, a large-area gauge adjustment is applied to the satellite-only estimate to ensure consistency in regions with sparse gauges. This large-area adjustment has the effect of exaggerating the influence of isolated island gauges on the surrounding open ocean grid boxes. Therefore, GPCC gauges from isolated island stations are not used in IMERG, which has the effect of ensuring that the PACRAIN atoll gauges are independent of IMERG. It is important to note that the PACRAIN atoll gauges, like any other gauge, are subject to undercatch but have no wind-loss correction, so they are likely low by approximately 5%–8% (J. Greene, University of Oklahoma, 2019, personal communication). Application of an appropriate wind-loss correction to the PACRAIN atoll gauges would increase the amount of monthly precipitation and push the mean of the adjusted atoll observations toward the mean of the IMERG estimates, possibly leading to an overall underestimation by IMERG. The detailed impact of undercatch on bias as a function of rain rate is a separate study in its own right.

Routine validation of satellite-based precipitation estimates, especially in challenging regions such as over open ocean, is critical to improving algorithms such as IMERG. It is believed this analysis will prove useful in further understanding the behavior of the IMERG high-end overestimation, and provide a path forward to improvements in future version of IMERG. This analysis also provides users with additional insight regarding the performance of IMERG V06B over open ocean in terms of rate-dependent biases compared to the atoll gauges. Users are encouraged to share the results of their validation efforts with the IMERG development team to assist in future improvements to the IMERG algorithm.

Acknowledgments. The authors wish to thank the reviewers for their insightful comments that improved this paper. We also wish to acknowledge Scott Greene and Ethan Cook of the University of Oklahoma for providing useful insight into the details of the PACRAIN data set.

Data availability statement. The IMERG data used in this study are openly available from the NASA Goddard Earth Sciences Data and Information Services Center at https://dx.doi.org/10.5067/GPM/IMERG/3B-MONTH/06 as cited in Huffman et al (2020). The PACRAIN data used in this study are openly available from the University of Oklahoma at https://pacrain.ou.edu as cited in Cook and Greene (2019).

REFERENCES

Bell, T. L., and P. K. Kundu, 2003: Comparing satellite rainfall estimates with rain gauge data: Optimal strategies suggested by a spectral model. *J. Geophys. Res.*, **108**, 4121, https://doi.org/10.1029/2002JD002641.

Bourlès, B., and Coauthors, 2008: The PIRATA Program. *Bull. Amer. Meteor. Soc.*, **89**, 1111–1126, https://doi.org/10.1175/2008BAMS2462.1.

Cook, W. E., and J. S. Greene, 2019: Gridded monthly rainfall estimates derived from historical atoll observations. *J. Atmos. Oceanic Technol.*, **36**, 671–687, https://doi.org/10.1175/JTECH-D-18-0140.1.

Gehne, M., T. M. Hamill, G. N. Kiladis, and K. E. Trenberth, 2016: Comparison of global precipitation estimates across a range of temporal and spatial scales. *J. Climate*, **29**, 7773–7795, https://doi.org/10.1175/JCLI-D-15-0618.1.

Gelaro, R., and Coauthors, 2017: The Modern-Era Retrospective Analysis for Research and Applications, version 2 (MERRA-2). *J. Climate*, **30**, 5419–5454, https://doi.org/10.1175/JCLI-D-16-0758.1.

Grecu, M., W. S. Olson, S. J. Munchak, S. Ringerud, L. Liao, Z. Haddad, B. L. Kelley, and S. F. McLaughlin, 2016: The GPM combined algorithm. *J. Atmos. Oceanic Technol.*, **33**, 2225–2245, https://doi.org/10.1175/JTECH-D-16-0019.1.

Greene, J. S., M. Klatt, M. Morrissey, and S. Postawko, 2008: The Comprehensive Pacific Rainfall Database. *J. Atmos. Oceanic Technol.*, **25**, 71–82, https://doi.org/10.1175/2007JTECHA904.1.

Hong, Y., K.-L. Hsu, S. Sorooshian, and X. Gao, 2004: Precipitation estimation from remotely sensed imagery using an artificial neural network cloud classification system. *J. Appl. Meteor.*, **43**, 1834–1853, https://doi.org/10.1175/JAM2173.1.

Huffman, G. J., and Coauthors, 2007: The TRMM Multisatellite Precipitation Analysis (TMPA): Quasi-global, multiyear, combined-sensor precipitation estimates at fine scales. *J. Hydrometeor.*, **8**, 38–55, https://doi.org/10.1175/JHM560.1.

——, R. F. Adler, D. T. Bolvin, and E. J. Nelkin, 2010: The TRMM Multi-satellite Precipitation Analysis (TMPA). *Satellite Rainfall Applications for Surface Hydrology*, F. Hossain and M. Gebremichael, Eds., Springer, 3–22.

——, and Coauthors, 2019: NASA Global Precipitation Measurement (GPM) Integrated Multi-satellitE Retrievals for GPM (IMERG). Algorithm Theoretical Basis Doc., version 6, 34 pp., https://gpm.nasa.gov/sites/default/files/document_files/IMERG_ATBD_V06.pdf.

——, and Coauthors, 2020: Integrated Multi-satellitE Retrievals for the Global Precipitation Measurement (GPM) mission (IMERG). *Satellite Precipitation Measurement*, V. Levizzani et al., Eds., Vol. 1, Advances Global Change Research, Vol. 67, Springer, 343–353, https://doi.org/10.1007/978-3-030-24568-9_19.

Joyce, R. J., J. E. Janowiak, P. A. Arkin, and P. Xie, 2004: CMORPH: A method that produces global precipitation estimates from passive microwave and infrared data at high spatial and temporal resolution. *J. Hydrometeor.*, **5**, 487–503, https://doi.org/10.1175/1525-7541(2004)005<0487:CAMTPG>2.0.CO;2.

——, P. Xie, and J. E. Janowiak, 2011: Kalman filter based CMORPH. *J. Hydrometeor.*, **12**, 1547–1563, https://doi.org/10.1175/JHM-D-11-022.1.

Khan, S., and V. Maggioni, 2019: Assessment of level-3 gridded Global Precipitation Mission (GPM) products over oceans. *Remote Sens.*, **11**, 255, https://doi.org/10.3390/rs11030255.

Kidd, C., 2018: NASA Global Precipitation Measurement (GPM) Precipitation Retrieval and Profiling Scheme (PRPS). Algorithm Theoretical Basis Doc., version 01-02, 16 pp., https://pps.gsfc.nasa.gov/Documents/20180203_SAPHIR-ATBD.pdf.

——, A. Becker, G. J. Huffman, C. L. Muller, P. Joe, G. Skofronick-Jackson, and D. B. Kirschbaum, 2017: So, how much of the Earth's surface is covered by rain gauges? *Bull. Amer. Meteor. Soc.*, **98**, 69–78, https://doi.org/10.1175/BAMS-D-14-00283.1.

Klepp, C., 2015: The oceanic shipboard precipitation measurement network for surface validation—OceanRAIN. *Atmos. Res.*, **163**, 74–90, https://doi.org/10.1016/j.atmosres.2014.12.014.

——, and Coauthors, 2017: Ocean Rainfall and Ice-Phase Precipitation Measurement Network—OceanRAIN-M. World Data Center for Climate (WDCC) at DKRZ, accessed 13 July 2020, https://doi.org/10.1594/WDCC/OceanRAIN-M.

Kucera, P., and C. Klepp, 2017: Validation of High Resolution IMERG Satellite Precipitation over the Global Oceans using OceanRAIN. *Geophysical Research Abstracts*, Vol. 19, Abstract 11794, https://meetingorganizer.copernicus.org/EGU2017/EGU2017-11794.pdf.

Kummerow, C., W. Barnes, T. Kozu, J. Shiue, and J. Simpson, 1998: The Tropical Rainfall Measuring Mission (TRMM) sensor package. *J. Atmos. Oceanic Technol.*, **15**, 809–817, https://doi.org/10.1175/1520-0426(1998)015<0809:TTRMMT>2.0.CO;2.

——, and Coauthors, 2001: The evolution of the Goddard Profiling Algorithm (GPROF) for rainfall estimation from passive microwave sensors. *J. Appl. Meteor.*, **40**, 1801–1820, https://doi.org/10.1175/1520-0450(2001)040<1801:TEOTGP>2.0.CO;2.

——, D. L. Randel, M. Kulie, N.-Y. Wang, R. Ferraro, S. J. Munchak, and V. Petkovic, 2015: The evolution of the Goddard profiling algorithm to a fully parametric scheme. *J. Atmos. Oceanic Technol.*, **32**, 2265–2280, https://doi.org/10.1175/JTECH-D-15-0039.1.

Legates, D. R., 1987: *A Climatology of Global Precipitation*. Publications in Climatology, Vol. 40, University of Delaware, 85 pp.

McPhaden, M. J., 1995: The Tropical Atmosphere Ocean array is completed. *Bull. Amer. Meteor. Soc.*, **76**, 739–744, https://doi.org/10.1175/1520-0477-76.5.739.

——, and Coauthors, 2009: RAMA: The Research Moored Array for African–Asian–Australian Monsoon Analysis and Prediction. *Bull. Amer. Meteor. Soc.*, **90**, 459–480, https://doi.org/10.1175/2008BAMS2608.1.

Morrissey, M. L., 1991: Using sparse raingages to test satellite-based rainfall algorithms. *J. Geophys. Res.*, **96**, 18 561–18 571, https://doi.org/10.1029/91JD01790.

Postawko, S., M. Morrissey, and B. Gibson, 1994: The Schools of the Pacific Rainfall Climate Experiment: Combining research and education. *Bull. Amer. Meteor. Soc.*, **75**, 1260–1266, https://doi.org/10.1175/1520-0477-75.7.1249.

Schneider, U., A. Becker, P. Finger, A. Meyer-Christoffer, and M. Ziese, 2018a: GPCC Monitoring Product: Near real-time monthly land-surface precipitation from rain-gauges based on SYNOP and CLIMAT data. DWD, accessed 24 July 2020, https://doi.org/10.5676/DWD_GPCC/MP_M_V6_100.

——; ——, ——, ——, and ——, 2018b: GPCC Full Data Monthly Product version 2018 at 1.0°: Monthly land-surface precipitation from rain-gauges built on GTS-based and historical data. DWD, accessed 24 July 2020, https://doi.org/10.5676/DWD_GPCC/FD_M_V2018_100.

Tan, J., G. J. Huffman, D. T. Bolvin, and E. J. Nelkin, 2019: IMERG V06: Changes to the morphing algorithm. *J. Atmos. Oceanic Technol.*, **36**, 2471–2482, https://doi.org/10.1175/JTECH-D-19-0114.1.

Taylor, R. C., 1973: An atlas of Pacific islands rainfall. Data Rep. 25, Dept. of Meteorology, University of Hawai'i at Mānoa, 174 pp.

Wu, Q., and Y. Wang, 2019: Comparison of oceanic multisatellite precipitation data from tropical rainfall measurement mission and global precipitation measurement mission datasets with rain gauge data from ocean buoys. *J. Atmos. Oceanic Technol.*, **36**, 903–920, https://doi.org/10.1175/JTECH-D-18-0152.1.